

# Analyzing the Optimal Matching of DC Motors to Photovoltaic Modules via DC-DC converters

Jesus Gonzalez-Llorente\*, Eduardo I. Ortiz-Rivera†, Andres Salazar-Llinas‡ and Emil Jimenez-Brea§

Department of Electrical and Computer Engineering

University of Puerto Rico at Mayaguez

Mayaguez, PR 00681-9042

jesus.gonzalez@ece.uprm.edu\*, eduardo.ortiz@ece.uprm.edu†, andres.salazar@ece.uprm.edu‡, emil.jimenez@ece.uprm.edu§

**Abstract**—Because to the nonlinear behavior of the photovoltaic (PV) cells, dc-dc power converters are added for matching the load to the photovoltaic modules (PVM). In this paper, we use mathematical models in order to examine the behavior of the off-grid photovoltaic system composed by: PV generator, dc-dc converter and dc motor. We compare different converter topologies (step-up, step-down and step-down/step-up) and evaluate the feasibility of being used as interface to attain operation around the maximum power point (MPP). Our analysis found the relationships between the optimal duty ratio and the maximum power, and between the optimal duty ratio and the motor speed; using these relationships, the simplest topology to meet the requirement can be selected as interface. Moreover, a simple but reliable maximum power point tracking (MPPT) method and a controller are implemented on a microcontroller and tested in real weather conditions. The MPPT provides an approximation to the optimal voltage or to the optimal current in a straightforward way, and the controller adjusts the duty ratio of the power converter, improving the matching of the PVM supplying a dc motor, when operation around MPP is obtained.

## I. INTRODUCTION

Since the photovoltaic (PV) generators are dc sources, these generators are very useful to supply dc motors. There are many applications of PV systems where the load is a dc motor, such as: refrigeration, telecommunication and water pumping, among others applications [1].

When a dc motor is directly connected to a photovoltaic module, the operating point of the PVM is very far from its maximum power point (MPP) [2], [3]. In order to improve the performance, the operating point must be closer to MPP; for this purpose is needed matching of the DC motor to the PVM. The matching could be reached by selecting carefully the dc motor according to motor I-V curve, mechanical load characteristics and PVM parameters [4]–[6], and by including an maximum power point tracker (MPPT) [2], [3], [7].

The interfacing circuit consists of dc-dc power converters, which can vary the current coming from the PV array; thus its duty ratio is adjusted to a value until optimal matching is achieved [8]. Step-down and step-up topologies such as nonisolated buck and boost dc-dc converters are widely used as photovoltaic interfaces due to their advantages of simplicity and efficiency [9].

Step-up dc-dc power converters were used as circuit interface between a PVM and a DC motor in [2], [3], [10]–[12], whereas in [13]–[17] step-down dc-dc converters were

employed. Furthermore, in [18], [19] step-down/step-up converter can be found. All of them utilized varied ways to adjust the duty ratio of power converter, but none of them specified the necessary conditions for optimal matching with the used topology. Thus, we studied different types of dc-dc converters, including step-up, step-down and step-down/step-up topologies in order to determine the conditions for attaining the matching.

We used an analytical method for comparing the different power converters, obtaining expression for the optimal duty ratio. Besides, this paper presents a schema with MPPT for the system consisted of PV array, dc-dc converter and dc motor, which can track the maximum power point without dependence on temperature, irradiance, or the kind of mechanical load. Finally, experimental results under real weather conditions are presented.

## II. INTERFACING THE PHOTOVOLTAIC MODULE TO THE DC MOTOR

Without any interfacing circuitry between the PVM and the dc motor, the operating point depends on the temperature, the irradiance, PVM specifications and the dc motor parameters. Then, if the dc motor characteristic I-V is superimposed on a set of photovoltaic I-V curves, the operating point is given by intersection between this curves [2]. The characteristics curves can be obtained by using the PV array and dc motor models, which are described below.

### A. Mathematical models

The relationship of the current ( $I$ ) with respect to the voltage ( $V$ ), for any PV array is given in (1). This model takes into consideration the short-circuit current ( $I_x$ ) and the open-circuit voltage ( $V_x$ ) at any given irradiance level ( $E_i$ ) and temperature ( $T$ ), the PVM characteristic constant ( $b$ ), and the numbers of in series and in parallels modules with the same electrical characteristics ( $s$  and  $p$ , respectively). The PVM exponential model is fully described in [20], [21].

$$I(V) = \frac{p \cdot I_x}{1 - \exp\left(\frac{-1}{b}\right)} \cdot \left[ 1 - \exp\left(\frac{V}{b \cdot s \cdot V_x} - \frac{1}{b}\right) \right] \quad (1)$$

Electrical side of a dc motor with constant field flux can be described for (2), and the torque balance equation is given by (3) [22].

$$V_a = R_a \cdot i_a + L_a \frac{di_a}{dt} + K_e \cdot \omega_m \quad (2)$$

$$T_e = J \cdot \frac{d\omega_m}{dt} + B_m \cdot \omega_m + T_L \quad (3)$$

In the above equations  $R_a$ ,  $L_a$ ,  $K_e$ ,  $V_a$  and  $i_a$  are armature resistance, armature inductance, back emf constant, armature voltage and current respectively.  $J$ ,  $B_m$ , and  $T_L$  are the moment of inertia of the motor and connected load, constant viscous friction coefficient and load torque, respectively. The electromagnetic torque,  $T_e$ , is proportional to the current through the armature winding and can be written as  $T_e = K_e \cdot i_a$ .

The PVM and DC motor  $I - V$  curves are illustrated in Fig. 1(a), where different operating points are shown according to the irradiance conditions and to the kind of dc motor load. Moreover, The dc motor  $P - V$  curves for different load characteristics, are superimposed on a set of PVM  $P - V$  curves for different irradiance in Fig. 1(b) [12]. It shows that for some load ( $T_L$ ) the motor voltage is always lower than PVM optimal voltage. The torque-speed characteristics of the load is given by  $T_L = c_1 \cdot \omega_m + c_2$ , where the constants  $c_1$  and  $c_2$  depend on the chosen position of the braking magnet of an eddy current brake.

As can be seen from Fig. 1, there is only few conditions where the operating point is near to the maximum power point in direct coupling. The operating point of the PV array can be moved to the maximum power point using a dc-dc converter as interface. This is possible, because the input resistance ( $R_i$ ) of a power converter in continuous conduction mode (CCM) depends on the duty ratio ( $D$ ) and the load resistance ( $R_o$ ) [23], [24]. Fig 2 shows the relationship between the normalized input resistance ( $R_i/R_o$ ) and the duty ratio  $D$  of power converter for CCM in steady state.

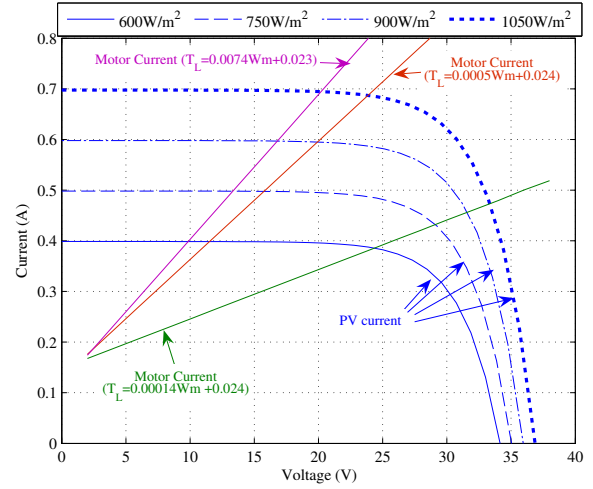
### III. OPTIMAL MATCHING WITH MPPT

This section describes the derivation of the optimal duty ratio for each one of the basic dc-dc power converter: step-down, step-up, and step-down/step-up. Since the optimal duty ratio depends on the voltage at maximum power of the PVM ( $V_{op}$ ), a simple mathematical method to approximate this method is shown.

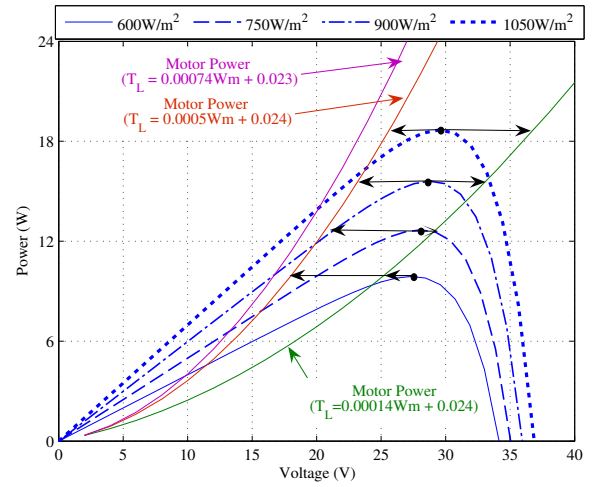
#### A. Derivation of the optimal duty ratio for each topology

For the buck chopper converter, shown in Fig. 3(a), the duty ratio is expressed by  $D = V_o/V_i$ ; the power converter output voltage  $V_o$  is equal to the motor armature voltage,  $V_a$ . The power converter input voltage  $V_i$  is equal to PVM voltage  $V$ , or equal to  $V_{op}$  if the terminal voltage of the PVM is operating in the maximum power point.

The optimal duty ratio can be obtained by substitution of  $V_a$  in  $D = V_a/V_{op}$ , where  $V_{op}$ , is the terminal voltage of the PVM corresponding to the maximum power point and  $V_a$ , in steady condition, is given by  $V_a = R_a \cdot I_a + K_e \cdot \omega_m$  [14]. Then the optimal duty ratio is given by (4):



(a) I-V curves DC motor and PVM



(b) Power curves DC motor and PVM

Fig. 1. PV and DC motor Curves

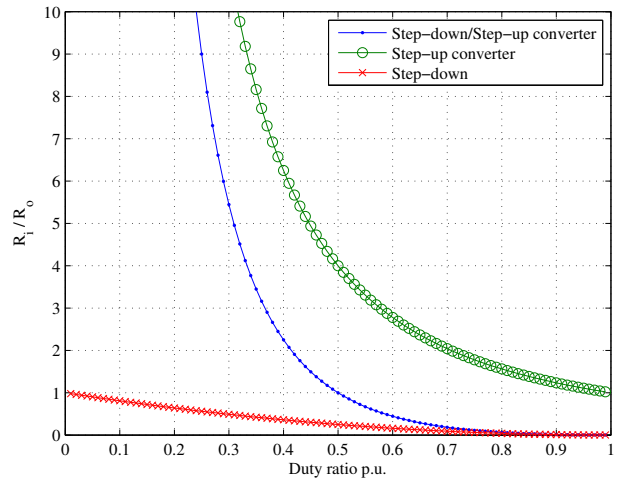


Fig. 2. Normalized input resistance in CCM of power converters

$$D = \frac{V_a}{V_{op}} = \frac{1}{V_{op}} \left[ K_e \cdot \omega_m + R_a \left( \frac{B_m \cdot \omega_m + T_L}{K_e} \right) \right] \quad (4)$$

For the Boost converter, shown in Fig. 3(b), whose output-to-input voltage conversion ratio, is given by

$$\frac{V_o}{V_{in}} = \frac{1}{1-D} \quad (5)$$

similar procedure is done, and from (6) optimal duty cycle is derived and shown in (7).

$$\frac{1}{1-D} = \frac{V_a}{V_{op}} = \frac{1}{V_{op}} \left[ K_e \cdot \omega_m + R_a \left( \frac{B_m \cdot \omega_m + T_L}{K_e} \right) \right] \quad (6)$$

$$D = 1 - \frac{K_e \cdot V_{op}}{K_e^2 \cdot \omega_m + R_a \cdot B_m \cdot \omega_m + T_L R_a} \quad (7)$$

The relationship of the input and the output voltage of the Buck-Boost, Cuk and SEPIC converter is given by

$$\frac{V_o}{V_{in}} = \frac{D}{1-D} \quad (8)$$

Fig. 3(c) shows a Buck-Boost converter as interface. If  $V_o = V_a$  and  $V_{in} = V_{op}$ , then, the optimal duty ratio can be derived from (9), and is given by (10)

$$\frac{D}{1-D} = \frac{V_a}{V_{op}} = \frac{1}{V_{op}} \left[ K_e \cdot \omega_m + R_a \left( \frac{B_m \cdot \omega_m + T_L}{K_e} \right) \right] \quad (9)$$

$$D = \frac{R_a \cdot B_m \cdot \omega_m + K_e^2 \cdot \omega_m + R_a \cdot T_L}{R_a \cdot B_m \cdot \omega_m + K_e^2 \cdot \omega_m + V_{op} \cdot K_e + R_a \cdot T_L} \quad (10)$$

Table I summarize the relationship between optimal the duty ratio and the motor speed for each topology. The optimal voltage  $V_{op}$  can be calculated by Linear Reoriented Coordinates Method (LRCM) [25].

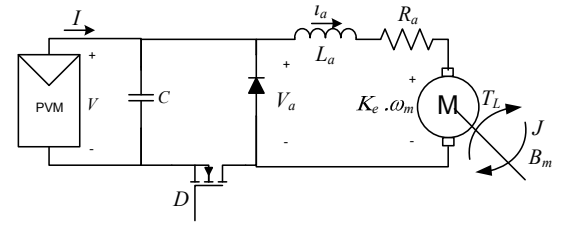
### B. Maximum power point tracking method

The Linear Reoriented Coordinates Method (LRCM) was proposed in [25], but the verification was based only in simulation results. This paper presents experimental verification applying a simpler equation to approximate the optimal voltage  $V_{op}$ , using the measurement of open-circuit voltage ( $V_x$ ) and the characteristic constant of PV array ( $b$ ).

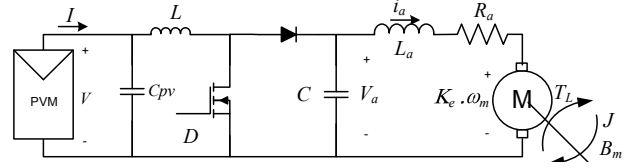
The equations of the approximated optimal voltage ( $V_{ap}$ ) and the approximated optimal current ( $I_{ap}$ ) are given by (11) and (12) respectively; however  $V_{ap}$  is preferable to track the MPP because the PVM voltage has a slower dynamics than the PVM current [9]. The MPPT is completed with the selected dc-dc converter and a PI controller that adjusts the power converter duty ratio in order to maintain the PVM voltage at its setpoint, which is given by ( $V_{ap}$ ).

$$V_{ap} = V_x + b \cdot V_x \cdot \ln \left( b - b \cdot \exp \left( -\frac{1}{b} \right) \right) \leq V_{op} \quad (11)$$

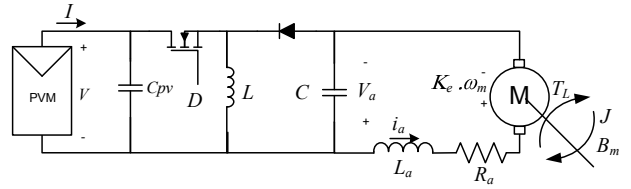
$$I_{ap} = I_x \cdot \frac{1 - b + b \cdot \exp \left( \frac{-1}{b} \right)}{1 - \exp \left( \frac{-1}{b} \right)} \geq I_{op} \quad (12)$$



(a) Step-down converter



(b) Step-up converter



(c) Step-down/Step-up converter

Fig. 3. Different power converters as interface

TABLE I  
SUMMARY OF OPTIMAL DUTY RATIO

Power converter	Optimal Duty Ratio
Step-down	$D = \frac{1}{V_{op}} \left[ K_e \cdot \omega_m + R_a \left( \frac{B_m \cdot \omega_m + T_L}{K_e} \right) \right]$
Step-up	$D = 1 - \frac{K_e \cdot V_{op}}{K_e^2 \cdot \omega_m + R_a \cdot B_m \cdot \omega_m + T_L R_a}$
Step-down/Step-up	$D = \frac{R_a \cdot B_m \cdot \omega_m + K_e^2 \cdot \omega_m + R_a \cdot T_L}{R_a \cdot B_m \cdot \omega_m + K_e^2 \cdot \omega_m + V_{op} \cdot K_e + R_a \cdot T_L}$

### C. Implementation of MPPT

Fig. 4 represents the proposed system using LRCM. The control system consisted of: ATMEL's ATmega88 8-bit microcontroller; interface circuits which comprise of sensors and signal conditioners connected to the analog-to-digital converter (ADC) of the microcontroller, and a driver for the power MOSFET.

The transistor Qv disconnects the PVM each time the LRCM is executed, allowing to measure the open-circuit voltage  $V_x$ . The voltage divider composed of  $R_1$  and  $R_2$  produces a fraction of the PVM voltage, which can be connected to the microcontroller ADC through a signal conditioner. This voltage is used to calculate the error with respect to the desired voltage  $V_{ap}$ .

The main program of the microcontroller only initialize its internal modules and wait for the timer overflow interruption. The interrupt routine executes the LRCM to update the setpoint, by disconnecting of the PVM at regular intervals and updating  $V_{ap}$ . Moreover, this routine uses a interrupt counter to obtain a constant sampling time for the controller.

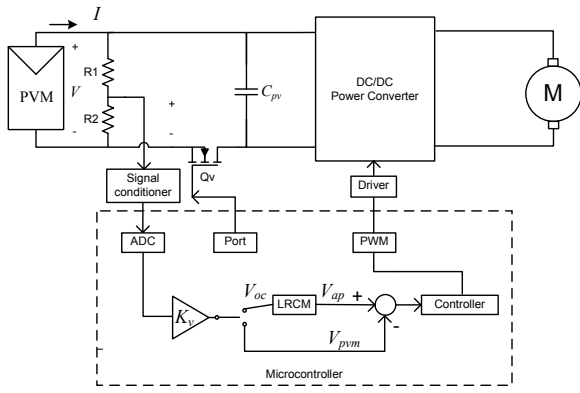


Fig. 4. Digital MPPT with LRCM

The control variable of a PI can be expressed by (13) in ideal form.

$$u(t) = K_p \left[ e(t) + \frac{1}{T_i} \int_0^{\infty} e(t) dt \right] \quad (13)$$

where  $u(t)$  is the output of the controller and  $e(t) = r(t) - y(t)$ , in which  $r(t)$  is the optimal voltage and  $y(t)$  is the actual voltage of the PVM.  $K_p$  and  $T_i$  are known as proportional gain and integral time respectively. The trapezoidal approximation for the integral term, which is also known as Bilinear transform or Tustin's method is used for discretization of (13), thus this becomes:

$$u(t_k) = K_p \cdot e(t_k) + K_i \left( \frac{e(t_k) + e(t_{k-1})}{2} \right) T_S + u(t_{k-1}) \quad (14)$$

#### IV. SIMULATION AND EXPERIMENTAL RESULTS

The systems is tested with a separately excited dc motor with constant field; therefore, the induced emf is proportional to the rotor speed, likewise in a permanent magnet dc motor. The motor parameters are listed in table II.

The motor is loaded through an eddy current brake, where the position of the braking magnet define the load torque ( $T_L$ ) applied. In this case the load torque is proportional to speed and it is given by  $T_L = c_1 \cdot \omega_m + c_2$ ; the constants  $c_1$  and  $c_2$  are calculated from real data and are shown in table III.

The PV array used for this study consist of two PVMs BP SX10M connected in series. The electrical characteristics of PVM BP SX10M are presented in table IV. The PVM characteristic constant is  $b = 0.084$  [12].

TABLE II  
DC MOTOR PARAMETERS

Symbol	Parameter	Value	Units
$R_a$	Armature resistance	8.57	$\Omega$
$L_a$	Armature inductance	58.7	$mH$
$K_e$	Back emf constant	0.1485	$\frac{V}{rad/sec}$
$J$	Moment of inertia	$45.5 \times 10^{-6}$	$Kg \cdot m^2$
$B_m$	Viscous friction coefficient	$94.8 \times 10^{-6}$	$\frac{N \cdot m}{rad/seg}$

TABLE III  
LOAD TORQUE CHARACTERISTIC FOR DIFFERENT POSITIONS,  
 $T_L = c_1 \cdot \omega_m + c_2$

Position	Constant $c_1$	Constant $c_2$
3	0.00014	0.024
4	0.00038	0.023
5	0.00055	0.024
6	0.00074	0.023

TABLE IV  
PVM BP SX10M SPECIFICATIONS AT STC

Symbol	Parameter	Value	Units
$I_{sc}$	Short-circuit Current	0.65	A
$V_{oc}$	Open-circuit Voltage	21.0	V
$P_{max}$	Maximum Power	10.0	W
$V_{op}$	Voltage at $P_{max}$	16.8	V
$I_{op}$	Current at $P_{max}$	0.59	A
$TC_i$	Temperature coeff. of $I_{sc}$	$(0.065 \pm 0.015)$	%/C
$TC_v$	Temperature coeff. of $V_{oc}$	$-(80 \pm 10)$	mV/C

#### A. Comparison of circuit interfacing

Using the derived expressions for the optimal duty ratio, which are shown in Table I, the relationship between optimal duty ratio and maximum power can be calculated for each studied topology. Therefore, it is possible evaluate this relationship at different loads in order to determine if the topology is suitable to extract the maximum power.

Fig. 5 shows the relationship between optimal duty ratio and maximum power at different irradiance values for step-down, step-up and step-up/step-down converters, likewise Fig. 6 shows the relationship between optimal duty ratio and maximum speed.

Since the duty ratio must be between 0.0 and 1.0 p.u. carefully selection of the topology should be done according to the kind of load; by example, a step-down converter is suitable to match the PVM and the DC motor if the load is set up to the position 4, where the load torque is  $T_L = 0.00038 \cdot \omega_m + 0.023$ .

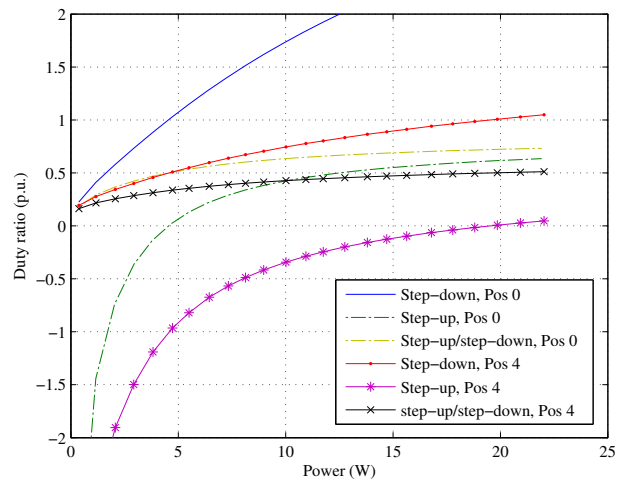


Fig. 5. Duty ratio vs Maximum power

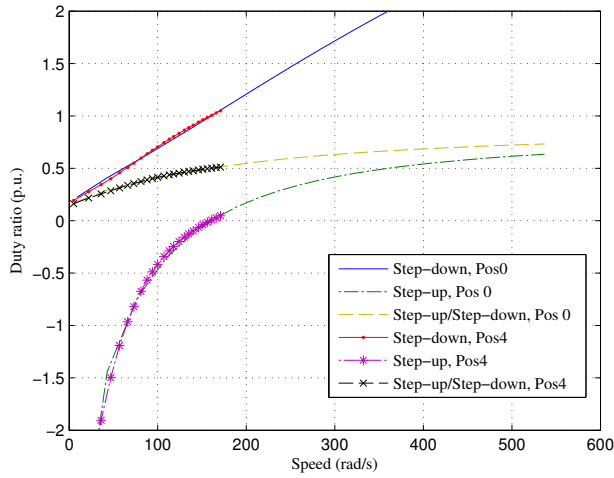
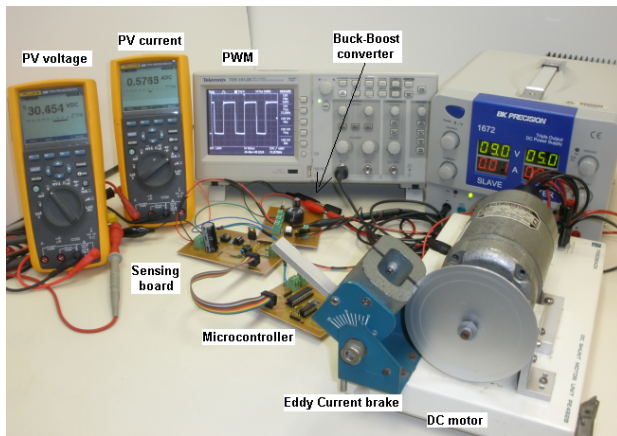


Fig. 6. Comparisons of optimal duty ratio for each topology



(a) System operation



(b) PV array

Fig. 7. Experiment setup

### B. Experimental Results with Step-down/step-up topology

Fig. 7 shows the experimental setup for the system, when the dc motor is used in shunt configuration; the motor started successfully while in direct coupling the dc motor did not start at the same environmental conditions.

The realized system was also tested with constant field for different weather conditions and constant torque load. Fig. 8 shows the PVM power, comparing the measured value with the theoretical value for different values of short-circuit current ( $I_x$ ) and open-circuit voltage ( $V_x$ ), which are shown in the top of each bar. Variations of irradiance and temperature produces the different values of  $I_x$  and  $V_x$ .

The method was also tested in real environmental conditions under load variations. The position of the braking magnet was changed in order to modify the load characteristics. The systems started with the braking magnet in the position 3; the position was modified each 25 seconds approximately, following the sequence: Position 3, position 5, position 4 and position 6.

Fig. 9 (top) shows the irradiance values and the output power of the PVM for the test condition. The average value of irradiance is equals to  $1134W/m^2$ . In spite of the variations of the load, the PV array kept providing the same power ( $15.6W$ ), shown in Fig. 9 (bottom). However, the disconnection of the PVM produces output power reduction, in “in press” [26] is shown how to estimate  $V_x$  without disconnection of the PVM.

The controller adjusted the duty ratio, which is shown in Fig. 10, keeping the PV array operating around of the maximum power point. The motor speed, shown in Fig.10 changed according to the load characteristics.

The PV array voltage and the PV array current are shown in Fig. 11. The load variations did not affect the performance of the MPPT method, the PV array voltage had a variation only of  $0.4V$  around of the approximated optimal voltage.

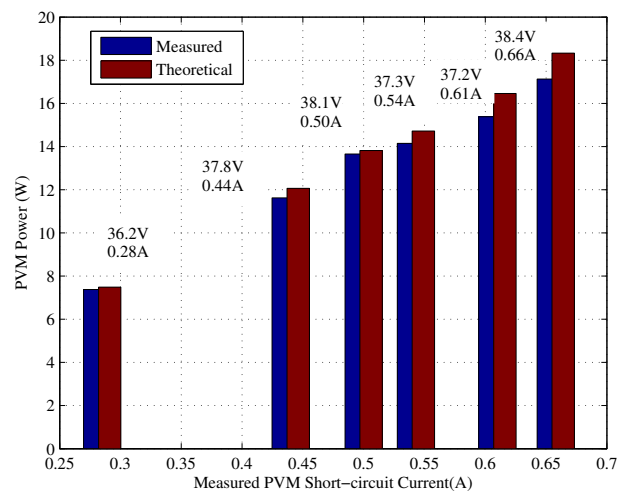


Fig. 8. PVM power at different environment conditions

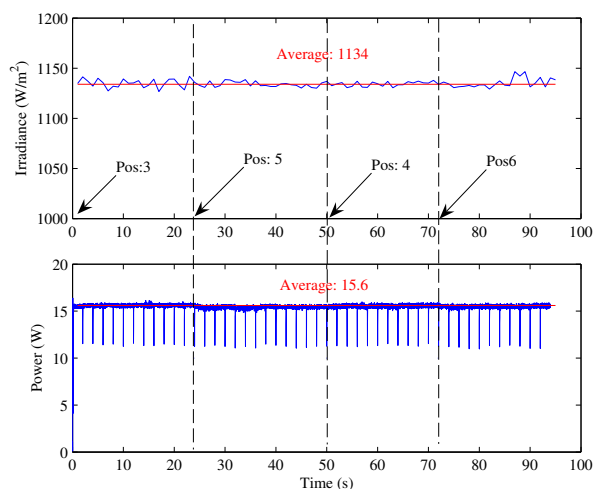


Fig. 9. Irradiance and PVM Power

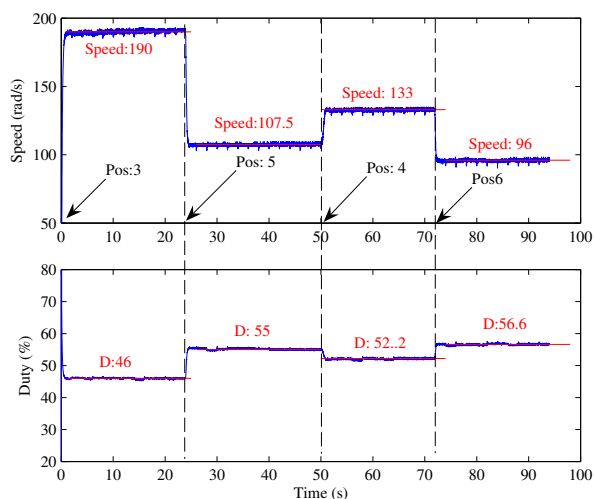


Fig. 10. Motor Speed and Duty ratio

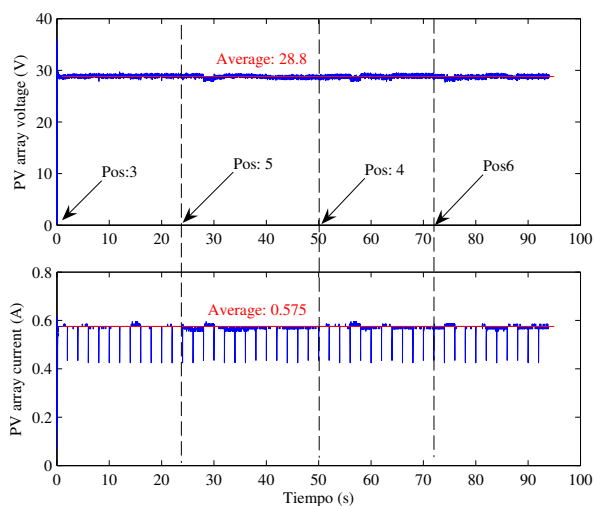


Fig. 11. PVM voltage and PVM current

## V. CONCLUSIONS

This paper presented a photovoltaic array feeding a dc motor; step-up, step-down and step-down/step-up dc/dc power converters were investigated as interface between PVM and the dc motor. Based on the mathematical model an expression for optimal duty ratio was derived for each dc/dc converter. Then, it showed the relationship between the optimal duty ratio and the maximum power point; as well as the relationship between the optimal duty ratio and the maximum speed. This comparative study allows to choose the suitable dc/dc power converter to supply a dc motor through a PVM. The analysis of the input resistance in steady state for the power converter was helpful to set up the action of the controller.

This paper also showed that it is possible to track the maximum power at different irradiance levels using the Linear Reoriented Coordinated Method (LRCM), only measurement of open-circuit voltage is required. When the load is changed, the LRCM keeps the PVM operating around the maximum power point in spite of variation of irradiance and temperature. A simplified method to track the maximum power point without iteration was shown. This method was implemented with the advantage of low cost and simple configuration. If the disconnection of the PV array were a unsuitable for the application. The LRCM could be implemented using irradiance measurement or a pilot PVM to estimate the open-circuit voltage.

## ACKNOWLEDGMENT

The authors gratefully acknowledge the contributions of all the members that belong to the Mathematical Modeling and Control of Renewable Energies for Advance Technology & Education ( $M_{inds}^2$  CREATE) Research Team at UPRM.

## REFERENCES

- [1] G. Masters, *Renewable and Efficient Electric Power Systems*. John Wiley & sons, Inc., 2004.
- [2] S. Alghuwainem, "Steady-state performance of dc motors supplied from photovoltaic generators with step-up converter," *Energy Conversion, IEEE Transaction on*, vol. 7, no. 2, pp. 267–272, Jun 1992.
- [3] —, "Matching of a dc motor to a photovoltaic generator using a step-up converter with a current-locked loop," *Energy Conversion, IEEE Transaction on*, vol. 9, no. 1, pp. 192–198, Mar 1994.
- [4] W. Fam and M. Balachander, "Dynamic performance of a dc shunt motor connected to a photovoltaic array," *Energy Conversion, IEEE Transaction on*, vol. 3, no. 3, pp. 613–617, Sep 1988.
- [5] M. Saied, "Matching of dc motors to photovoltaic generators for maximum daily gross mechanical energy," *Energy Conversion, IEEE Transaction on*, vol. 3, no. 3, pp. 465–472, Sep 1988.
- [6] —, "A study on the matching of dc motors to photovoltaic solar arrays," *Electrical Machines and Systems, 2001. ICEMS 2001. Proceedings of the Fifth International Conference on*, vol. 1, pp. 652–655 vol.1, 2001.
- [7] S. Singer and J. Appelbaum, "Starting characteristics of direct current motors powered by solar cells," *Energy Conversion, IEEE Transaction on*, vol. 8, no. 1, pp. 47–53, Mar 1993.
- [8] T. Eswam and P. Chapman, "Comparison of photovoltaic array maximum power point tracking techniques," *Energy Conversion, IEEE Transaction on*, vol. 22, no. 2, pp. 439–449, June 2007.

- [9] W. Xiao, W. G. Dunford, P. R. Palmer, and A. Capel, "Regulation of photovoltaic voltage," *Industrial Electronics, IEEE Transactions on*, vol. 54, no. 3, pp. 1365–1374, June 2007.
- [10] K. Hussein, I. Muta, T. Hoshino, and M. Osakada, "Field and armature control for separately excited dc motors powered by photovoltaic cells," *Photovoltaic Energy Conversion, 1994., Conference Record of the Twenty Fourth. IEEE Photovoltaic Specialists Conference - 1994, 1994 IEEE First World Conference on*, vol. 1, pp. 1169–1172 vol.1, Dec 1994.
- [11] M. Akbaba, "Optimization of the performance of solar powered permanent magnet dc motor drives," *Electrical Machines and Power Electronics, 2007. ACEMP '07. International Aegean Conference on*, pp. 725–729, Sept. 2007.
- [12] J. Gonzalez-Llorente, E. I. Ortiz-Rivera, and A. Diaz, "A maximum power point tracker using positive feedforward control based on the dc motor dynamics and pvm mathematical model," in *Electric Machines and Drives Conference, 2009. IEMDC '09. IEEE International, May 2009*, pp. 259–264.
- [13] S. Shokrolla, N. Twieg, and A. Sharaf, "A photovoltaic powered separately excited dc motor drive for rural/desert pump irrigation," *Electrical Machines and Drives, 1993. 6th International Conf. on*, pp. 406–411, Sep 1993.
- [14] K. Venkatesan and D. Cheverez-Gonzalez, "Matching dc motors to photovoltaic generators for maximum power tracking," *Applied Power Electronics Conf. and Exp. APEC '97 Conf. Proc. 1997., 12th Annual*, vol. 1, pp. 514–519 vol.1, Feb 1997.
- [15] A. Tariq and M. Asghar, "Matching of a separately excited dc motor to a photovoltaic panel using an analog maximum power point tracker," *Industrial Technology, 2006. ICIT 2006. IEEE International Conf. on*, pp. 1020–1025, Dec. 2006.
- [16] A. Sharaf and L. Yang, "A novel maximum power tracking controller for a stand-alone photovoltaic dc motor drive," *Electrical and Computer Engineering, 2006. CCECE '06. Canadian Conference on*, pp. 450–453, May 2006.
- [17] A. Sharaf, E. Elbakush, and I. Altas, "An error driven pid controller for maximum utilization of photovoltaic powered pmc motor drives," *Electrical and Computer Eng., 2007. CCECE 2007. Canadian Conf. on*, pp. 129–132, April 2007.
- [18] A. Hussein, K. Hirasawa, J. Hu, and J. Murata, "The dynamic performance of photovoltaic supplied dc motor fed from dc-dc converter and controlled by neural networks," *Neural Networks, 2002. IJCNN '02. Proceedings of the 2002 International Joint Conference on*, vol. 1, pp. 607–612, 2002.
- [19] E. E. Jimenez-Toribio, A. A. Labour-Castro, F. Muniz-Rodriguez, H. R. Perez-Hernandez, and E. I. Ortiz-Rivera, "Sensorless control of sepic and cuk converters for dc motors using solar panels," in *Electric Machines and Drives Conference, 2009. IEMDC '09. IEEE International, May 2009*, pp. 1503–1510.
- [20] O. Gil-Arias and E. I. Ortiz-Rivera, "A general purpose tool for simulating the behavior of pv solar cells, modules and arrays," *Control and Modeling for Power Electronics, 2008. COMPEL 2008. 11th Workshop on*, pp. 1–5, Aug. 2008.
- [21] E. Ortiz-Rivera and F. Peng, "Analytical model for a photovoltaic module using the electrical characteristics provided by the manufacturer data sheet," *Power Electronics Specialists Conf., 2005. PESC '05. IEEE 36th*, pp. 2087–2091, Sept. 2005.
- [22] R. Krishnan, *Electric Motor Drives: Modeling, Analysis and Control*. Prentice-Hall, 2001.
- [23] E. Ortiz-Rivera, "Maximum power point tracking using the optimal duty ratio for dc-dc converters and load matching in photovoltaic applications," in *Applied Power Electronics Conference and Exposition, 2008. APEC 2008. Twenty-Third Annual IEEE*, Feb. 2008, pp. 987–991.
- [24] E. Duran, M. Sidrach-de Cardona, J. Galan, and J. Andujar, "Comparative analysis of buck-boost converters used to obtain iv characteristic curves of photovoltaic modules," in *Power Electronics Specialists Conference, 2008. PESC 2008. IEEE*, June 2008, pp. 2036–2042.
- [25] E. rtiz Rivera and F. Peng, "A novel method to estimate the maximum power for a photovoltaic inverter system," *Power Electronics Specialists Conf., 2004. PESC 04. IEEE 35th Annual*, vol. 3, pp. 2065–2069 Vol.3, 20–25 June 2004.
- [26] E. Jimenez-Brea, A. Salazar-Llinas, E. Ortiz-Rivera, and J. Gonzalez-Llorente, "A maximum power point tracker implementation for photovoltaic cells using dynamic optimal voltage tracking," in *Applied Power Electronics Conference and Exposition, 2010. APEC 2010. Twenty-Fifth Annual IEEE*, in press.